High-Frequency Limit of 15.1-MeV Bremsstrahlung*†

H. E. HALL,‡ A. O. HANSON, AND D. JAMNIK§
Physics Department, University of Illinois, Urbana, Illinois
(Received 12 October 1962)

The 15.1-MeV scattering resonance in carbon is used to study the yield of photons at the high-frequency limit of the bremsstrahlung spectrum. A survey of the yield at 0° was carried out for several elements. The 0° yield at the limit increases strongly with the atomic number in agreement with recent calculations. Measurements of the 15.1-MeV isochromats from a thin thorium ($Z=90$) target for several angles are presented and compared with available calculations. A value of 1.61 ± 0.16 mb is obtained for $(k/Z^2)(d\sigma/dk)$, the cross section integrated over angle. This is in reasonable agreement with theoretical values of 1.96 mb based on the inverse photoeffect and 1.74 mb as obtained from a direct evaluation of the bremsstrahlung matrix element in the extreme relativistic limit.

I. INTRODUCTION

THE bremsstrahlung spectrum near the high-frequency limit continues to be of considerable interest since many experiments depend on a knowledge of the spectrum shape for the interpretation of photonuclear reactions, particularly near the upper limit. The problem of calculating the shape correctly is very complicated and has been completely carried out only for a few isolated points.

An extensive series of measurements of thin target bremsstrahlung produced by electrons up to 9.7 MeV was made by Starfelt and Koch[1] and more recently by Fuller, Hayward, and Koch[2] using the elastic scattering of 15.1-MeV photons by the C^{12} resonance as isochromat selector. Although the interpretation of the work near 15.1 MeV was difficult because of the experimental arrangement, the data indicated a definite excess of photons at the high-energy limit or "tip."

The increased interest in the bremsstrahlung tip spectrum has also brought about recent advances in theory. Fano[3] introduced detailed balance between the photoelectric and bremsstrahlung cross sections to obtain the cross section at the high-frequency limit. An excellent summary of previous work is presented by Koch and Motz.[4]

The experimental work on the high-frequency limit of the high-energy bremsstrahlung spectrum carried out at the University of Illinois[5] was divided into two distinct parts. The first was a survey of the 15.1-MeV isochromat at the tip for elements of different atomic number. This investigation was made using only the forward (0°) beam. These data present very clear evidence for the finite differential cross section at the tip and for a strong Z dependence but a detailed interpretation depends sensitively on the angular distribution assumed for the radiation from an infinitesimally thin target and the averaging over this angular distribution carried out by multiple scattering.

The second part was designed to investigate more completely the bremsstrahlung shape at the tip, as well as its angular distribution. A search was also made to see if the x rays at the tip might be strongly polarized.

The total yield (integrated over angle) at the tip was measured and is compared with calculations. The experimentally observed yield is significantly above that calculated from the Bethe-Heitler formula not only at the tip but also for energies of one or two MeV below the high-frequency limit.

II. THEORY

A. Bremsstrahlung Tip

In the high-frequency or "tip" region of the electron bremsstrahlung spectrum almost all of the energy of the incident electron is radiated leaving a low-energy outgoing electron ($\beta\sim0$). The very fact that the outgoing electron is of low energy invalidates the approach of Olson and Maximon[6] who use Sommerfeld-Maue wave functions and neglect terms of order of mc^2/E, where E is total energy of the outgoing electron. The approach of Bethe-Heitler,[7] which involves the Born approximation, is also invalid since it entails an expansion in $Z/137\beta_0$ and $Z/137\beta$, where β_0 and β are the velocities in units of c, for the incoming and outgoing electrons, respectively. Fano[8] noted that, in the Sauter[9] approximation, detailed balancing arguments

* Some of the work reported here was presented by H. E. Hall in partial fulfillment of the requirements for a Ph.D. degree in Physics.

† This work was supported in part by the joint program of the U. S. Office of Naval Research and the U. S. Atomic Energy Commission.

‡ Present address: General Electric Space Sciences Laboratory, King of Prussia, Pennsylvania.

§ Visitor physicist, now returned to Institut J. Stefan, Ljubljana, Yugoslavia.

[1] N. Starfelt and H. W. Koch, Phys. Rev. **102**, 1958 (1956).

[2] E. G. Fuller, E. Hayward, and H. W. Koch, Phys. Rev. **109**, 630 (1958).

[3] U. Fano, H. W. Koch, and J. W. Motz, Phys. Rev. **112**, 1679 (1958); referred to as F.K.M.

[4] H. W. Koch and J. W. Motz, Rev. Mod. Phys. **31**, 920 (1959).

[5] This work was the subject of Technical Report No. 26 issued by the Department of Physics (June 1961) and was presented at a meeting of the American Physical Society [Bull. Am. Phys. Soc. **6**, 434 (1961)].

[6] H. Olson and L. C. Maximon, Phys. Rev. **114**, 887 (1959).

[7] W. Heitler, *Quantum Theory of Radiation* (Oxford University Press, New York, 1954), 3rd ed., p. 242, ff.

[8] U. Fano, Phys. Rev. **116**, 1156 (1959).

[9] F. Sauter, Ann. Physik **9**, 217 (1931); **11**, 545 (1931). See also H. A. Bethe and E. Saltpeter, in *Encyclopedia of Physics*, edited by S. Flügge (Springer-Verlag, Berlin, 1957), Vol. 35, 398.

can be used to relate the tip cross section to the photoelectric cross section for the K shell.

In the Sauter approximation which is first order in $Z/137$, the bound and free-state wave functions are identical except for the normalization constant since one neglects the binding energy of the electron which is of the order of $(Z/137)^2$. Thus, in this approximation the photoelectric process is the inverse of x-ray emission at the high-frequency limit. This correspondence was considered in detail by McVoy and Fano[10] who demonstrate that the bremsstrahlung matrix elements are the same as the corresponding photoelectric matrix elements except for the factor $137/m^{1/2}Z$ which they derive in this approximation from the normalization factors.

Using their result, the photoelectric cross section σ_p, for the absorption of photons of energy k, and tip bremsstrahlung cross section $d\Phi_B/dk$ are related, to lowest order in $Z/137$, as follows:

$$\sigma_p=\alpha^2Z^2mc^2\frac{E_0+mc^2}{E_0-mc^2}\left(\frac{d\Phi_B}{dk}\right), \tag{1}$$

where $\alpha=1/137$, mc^2 is the electron rest energy, and E_0 is the total electron energy. The factor $(E_0+mc^2)/(E_0-mc^2)$ arises from the replacement of the density of states available for bremsstrahlung emission with the correct expression for the photoeffect. By substituting the appropriate form of the photoelectric cross section one may obtain differential or integral bremsstrahlung cross sections at the high-frequency limit. A relation for the cross section for the K-shell photoeffect in the extreme relativistic region was derived by Hall,[11] by Prange and Pratt,[12] and by Erber.[13] Hall made an approximate evaluation of the integrals involved which was shown to be incorrect by several authors.[13–17] Gavrila evaluated the integrals by an iterative process up to terms in the second order, obtaining the relation

$$\sigma_K=\sigma_K{}^0[1-\pi\alpha Z-(4/15)\pi\alpha Z], \tag{2}$$

where

$$\sigma_K{}^0=4\pi r_0{}^2\alpha^4Z^5/k \quad \text{and} \quad r_0=e^2/mc^2.$$

Later, by means of higher order Born approximations for the wave function, Gavrila[15] obtained an energy dependence for the differential and integral cross sections and showed that the integral cross section reduces to the form of Hall for the extreme relativistic case (exact in αZ) by letting $\beta\rightarrow 1$ and keeping only the lowest power of $(1-\beta^2)Z$.

Pratt[18] has made the most recent calculation of the K-shell photoeffect using the high-energy limit of the exact wave function. He made numerical calculations and also obtained the following approximate formula for the charge dependence:

$$\sigma_K(Z,\infty)=\sigma_K(\alpha Z)^{2\xi}[1-(4\pi/15)\alpha Z]\times\exp(2\alpha Z\cos^{-1}\alpha Z), \tag{3}$$

where

$$\xi=-1+(1-\alpha^2Z^2)^{1/2}\approx\alpha^2Z^2/2.$$

Numerical values from this formula are given, along with those calculated by the numerical work, in Table I of his work.[18] Combining his work with that of Gavrila, Pratt obtains an energy dependence expressed in terms of β by the relation:

$$\sigma(Z,E)=\sigma_K{}^0\frac{\beta^3}{k^4(1-\beta^2)^{3/2}}(\alpha Z)^{2\xi}M(\beta)\times\exp\left(-2\frac{\alpha Z}{\beta}\cos^{-1}\alpha Z\right)\left(1-\pi\alpha Z\frac{N(\beta)}{M(\beta)}+\cdots\right), \tag{4}$$

where $M(\beta)$ and $N(\beta)$ are the integrals given by Gavrila.[15]

In a subsequent article[19] Pratt derived an expression for the "L"-shell contribution to the photoelectric effect and showed that it was not negligible in the case of the heavier elements. The correspondence between the bremsstrahlung and the photoelectric cross sections was also shown to be valid to the next order of αZ and over a finite energy region near the limit.[20] He showed that the terms in the power series expansion of the wave function which contribute in lowest order are the same for the two processes (apart from normalization).

For convenience Pratt writes the photoeffect cross sections as

$$\sigma_p{}^J=\sigma_K{}^0[P^J(E)/P^J(\infty)]P^J(\infty), \tag{5}$$

where $\sigma_K{}^0$ as defined above is the high-energy, small-Z limit of the K-shell cross section, $P^J(E)/P^J(\infty)$ represents the energy dependence of the cross section, and $P^J(\infty)$ contains the Z dependence in the high-energy limit. J indexes the quantum numbers of the states. Writing the bremsstrahlung cross section at the tip in a similar manner and making use of the fact that the approximate connection between photoeffect and bremsstrahlung is the same for all shells he writes the following expression for the bremsstrahlung cross section:

$$d\Phi_B/dk=\sum_J\sigma_B{}^J=\sigma_B{}^0[P(E)/P(\infty)]B(\infty),$$

[10] K. W. McVoy and U. Fano, Phys. Rev. **116**, 1168 (1959).
[11] H. Hall, Rev. Mod. Phys. **8**, 358 (1936), Phys. Rev. **84**, 167 (1951).
[12] R. D. Prange and R. H. Pratt, Phys. Rev. **108**, 139 (1957).
[13] T. Erber, Ann. Phys. **6**, 319 (1959); also T. Erber and R. H. Pratt, Bull. Am. Phys. Soc. **3**, 368 (1958), and T. Erber (to be published).
[14] F. G. Nagasaka, Ph.D. thesis, University of Notre Dame, 1955 (unpublished); also F. G. Nagasaka and E. Guth, Bull. Am. Phys. Soc. **4**, 13 (1959).
[15] M. Gavrila, Phys. Rev. **113**, 514 (1959); also Nuovo Cimento **9**, 327 (1958).
[16] R. H. Boyer, Ph.D. thesis, University of Oxford, 1957 (unpublished), also Phys. Rev. **117**, 475 (1960).
[17] H. Banerjee, Nuovo Cimento **10**, 863 (1958); **11**, 220 (1959).
[18] R. H. Pratt, Phys. Rev. **117**, 1017 (1960).
[19] R. H. Pratt, Phys. Rev. **119**, 1619 (1960).
[20] R. H. Pratt, Phys. Rev. **120**, 1717 (1960).

where

$$B(\infty)=\sum_J B^J(\infty), \tag{6}$$

and $\sigma_B{}^J$ is the partial cross section of electrons of angular momentum J, and where $\sigma_B{}^0=(4\pi r_0{}^2\alpha^2Z^3/k)\times[(E-1)/(E+1)]$ is the low-Z high-energy limit of the bremsstrahlung cross section. Using only S and P states, $B(\infty)$ can be expressed as

$$B(\infty)=P^{1S}(\infty)+(32/3)[P^{2P_{1/2}}(\infty)+P^{2P_{3/2}}(\infty)]. \tag{7}$$

The values of $P(\infty)$ and $P(E)$ for the K shell are obtainable from Table II, reference 18, or from the ratio of Eqs. (3) and (4), while the values for $B(\infty)$ are given in Table I of reference 20. The tip cross section for a wide range of energies and atomic numbers can easily be obtained using these tables. The calculated values were expected to be accurate only within 20 to 30% for the heavy elements. The tip cross section obtained for different atomic numbers at 15.1 MeV is shown in Fig. 1 with several experimental results.

A more direct treatment of the bremsstrahlung cross section at the high-frequency limit has been made by Johnson and Mullin[21] and by Deck, Mullin, and Hammer[22] who consider the radiation by electrons with energies much greater than the rest mass.

They find an expression for the cross section, differential in angle and in photon energy, which when integrated over angles can be expressed as a correction to the first-order formula obtained by Fano, namely,

$$\frac{d\phi_B}{dk}=\sigma_B{}^0F(\gamma)e^{-\pi\alpha Z}\left\{1-\frac{4\pi}{15}\alpha Z+\left[\frac{23}{9}-\frac{139\pi^2}{720}\right](\alpha Z)^2\right\}, \tag{8}$$

where

$$F(\gamma)=\frac{4[\Gamma(\gamma)]^2}{[\Gamma(2\gamma+1)]^2}(2\alpha Z)^{2\gamma-2},$$

and

$$\gamma=(1-\alpha^2Z^2)^{1/2}.$$

Values from this expression for the tip cross section are shown in Fig. 1 as the lowest of the three curves. In order to make this expression applicable to lower energies, such as 15.1 MeV, the expression can be multiplied by the Z-dependent energy factor $[P(E)/P(\infty)]$ used by Pratt. When modified in this manner, the function is raised as shown by the dotted line which can be seen to be in reasonable agreement with the curve of Pratt.

B. Angular Distributions of the Photons

The angular distributions of the photons at the high-frequency limit given by the differential form of the various cross-section calculations based on the K-shell photoeffect are dominated by the terms such as $\sin^2\theta/(1-\beta\cos\theta)^4$ which give no intensity in the forward direction.

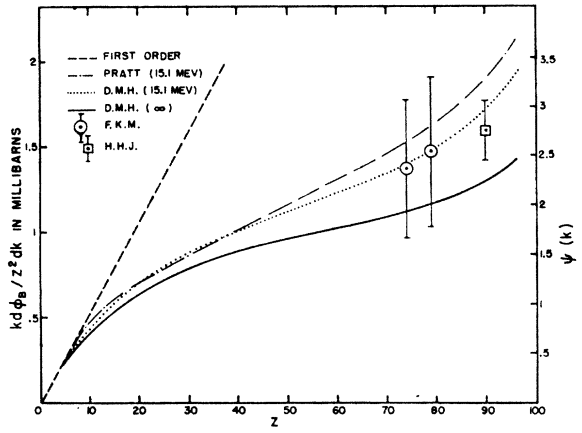

FIG. 1. The integrated over angle cross section for the production of photons at the high-frequency limit as a function of Z. The upper dashed line represents the first-order approximation of Fano; the broken line, the calculation of Pratt; the solid line, the expression of Deck, Mullin, and Hammer; and the dotted line, the same adjusted to 15.1 MeV according to the energy dependence given by Pratt. The ordinate on the right is expressed in units of $\alpha r_0{}^2$, namely, $\psi=(1/\alpha r_0{}^2)(kd\phi_B/Z^2dk)$. The circles represent the data of Fano, Koch, and Motz while the square represents the value for thorium obtained in this work.

The Sauter-Fano[9] distribution is similar and is the same for all Z, since the Z^3 dependence given by this theory does not perturb the shape of the angular distribution. The distribution for the K-shell photoeffect as calculated by Gavrila[15] is slightly Z dependent but still has no contribution in the forward direction.

Gavrila[23] has also calculated the differential cross section for the various "L"-shell contributions to the photoeffect which, by the inverse relation, apply to the bremsstrahlung process at the tip. These angular distributions are given in Fig. 2, where $L_{\rm I}$ is the distribution for transitions from the $2S_{1/2}$ state, $L_{\rm II}$ is for the $2P_{1/2}$ state, and $L_{\rm III}$ is for the $2P_{3/2}$ state. $L_{\rm I}$ is identical with the K-shell differential cross section except for an amplitude factor making it $\frac{1}{8}$ of the K-shell value at each point. The relative contributions of $L_{\rm II}$, $L_{\rm III}$, and S transitions to total yield was calculated by Pratt and are available from Table I of his article on bremsstrahlung.[20] It can be seen that the $L_{\rm II}$ contribution is negligible for low Z but important for high Z. In particular for a thorium target, $Z=90$, it is about 30% of the total yield. Since this yield is confined to a small angle the normalization makes its value at 0° about five times the maximum value for S transitions. The weighted average results in a strong maximum in the forward direction as is shown in Fig. 2. Angular distributions for other values of Z are shown in Fig. 3.

Another expression for the angular distribution which also gives a forward yield is available from the work of

[21] W. R. Johnson and C. J. Mullin, Phys. Rev. **119**, 1270 (1960).
[22] R. T. Deck, C. J. Mullin, and C. L. Hammer (to be published); referred to as D.M.H.
[23] M. Gavrila, Zh. Experim. i Teor. Fiz. **38**, 309 (1960) [translation: Soviet Phys.—JETP **11**, 224 (1960)]; Phys. Rev. **124**, 1132 (1961).

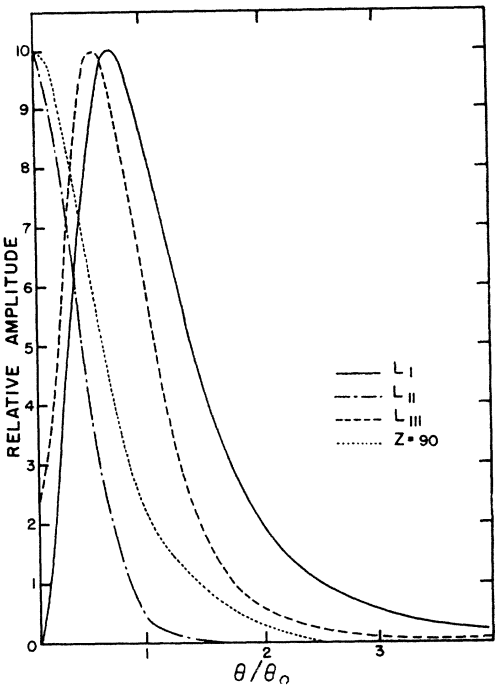

FIG. 2. Angular distributions of photoelectrons as calculated by Gavrila for transitions from the $2S_{1/2}$, $2P_{1/2}$, and $2P_{3/2}$ levels, respectively. The sum of these curves weighted according to the strength of these transitions in thorium is shown as $Z=90$.

Deck, Mullin, and Hammer. It includes terms in αZ and in $(\alpha Z)^2$ and gives similar angular distributions. These are shown in Fig. 4 and differ in that there are somewhat larger forward yields for intermediate values of Z.

C. Polarization

Another aspect of bremsstrahlung which is often of interest is the polarization. A number of calculations have been made and explicit evaluations were made by Gluckstern and Hull,[24] Fronsdal and Überall,[25] and by Motz and Placious.[26] These calculations are supported for the energy region considered here by the experimental results of Jamnik and Axel.[27] The calculations predict a negligible polarization at the tip. The approximations used, however, are not clearly valid at the tip even though the calculations agree with observations for 0.5-MeV electrons.[26,28]

[24] R. L. Gluckstern and M. M. Hull, Jr., Phys. Rev. **90**, 1030 (1953).

[25] C. Fronsdal and H. Überall, Nuovo Cimento **8**, 163 (1958); Phys. Rev. **111**, 580 (1958). Numerical results, transmitted to us by P. Axel, were obtained from the IBM 704 Computer in Paris using a CERN 2 program devised by Fronsdal and Überall.

[26] J. W. Motz and R. C. Placious, Nuovo Cimento **15**, 571 (1960).

[27] D. Jamnik and P. Axel, Phys. Rev. **117**, 194 (1960).

[28] J. W. Motz and R. C. Placious, Phys. Rev. **112**, 1039 (1958). An explicit discussion of the polarization correlations, as well as the transfer of helicity, at the tip is given by R. H. Pratt, *ibid.* **123**, 1508 (1961).

III. EXPERIMENTAL ARRANGEMENT AND PROCEDURE

A. Special Arrangements in the Betatron

This experiment was performed using the University of Illinois 22-MeV betatron with the thin target donut, originally constructed for the work with bremsstrahlung polarization by Jamnik and Axel which has been described in some detail.[27] It was shown that a beam stopper placed at about 180 deg from the target and within 1 mm of the radial position of the target was effective in preventing multiple traversals through the target as indicated by the reduction in the width of the angular distribution of bremsstrahlung.

The same technique was used in this work. Intensity angular distributions were measured for various relative radial positions of the beam stopper and an iterative procedure was used to determine positions giving distributions of minimum width consistent with a good central intensity. The angular distributions were measured by a remotely controlled lead covered ionization chamber, $\frac{1}{4}$ in. in diameter, subtending an angle of 0.0067 rad or 0.2 mc^2/E_0.

A series of angular distributions taken at different times with the aluminum and the thorium targets are shown in Fig. 5. The solid lines represent the calculated angular distributions expected for different thicknesses as indicated by the parameter m used by Miller.[27,29]

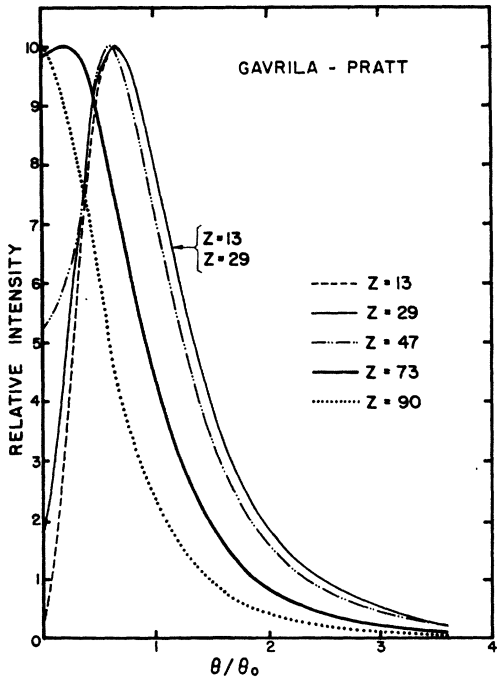

FIG. 3. The angular distributions of photoelectrons, or of tip bremsstrahlung, using the angular distributions of Gavrila weighted according to the contributions to the total yield as calculated by Pratt.

[29] J. Miller, Centre d'Etudes Nucléaires de Saclay Report CEA No. 655 (unpublished).

It is assumed that the photons from the target have a distribution associated with multiple scattering which can be expressed as an exponential integral

$$[\mathrm{Ei}(-\theta^2/2m^2\theta_0^2)],$$

and that the intrinsic angular distribution is given by the approximate formula of Schiff.[4] The parameter m is defined in terms of the root mean square multiple scattering in units of θ_0, namely, $m=\langle\theta_s^2\rangle^{1/2}/\sqrt{2}\theta_0$. It can be seen that the aluminum data fit very closely the curve for $m=\frac{1}{2}$ while that for thorium corresponds to $m=1$. Similar angular distributions were obtained for Cu, Pd, and Ta corresponding to $m=0.75$, 0.66, and 0.94, respectively. These m values were larger than those calculated from the target thicknesses by factors of 1.5 to 2.

B. Orbit Expansion

There are two modes of orbit expansion used with the 22-MeV betatron at the University of Illinois; they are the so-called "long"[30] and "short" pulse operations. In each case the orbit is caused to expand by a pulse of current through a single loop of wire above and below the orbit, this current pulse being of such a magnitude as to be able to deliver the beam to an orbit well beyond the target position.

The short-pulse mode gives a yield pulse of approximately 1 μsec duration and is initiated either by an integrator circuit or by a variable delay circuit. The integrator circuit has the advantage of giving better energy control than the variable delay circuit. A stability within ± 30 keV was obtained during these experiments.

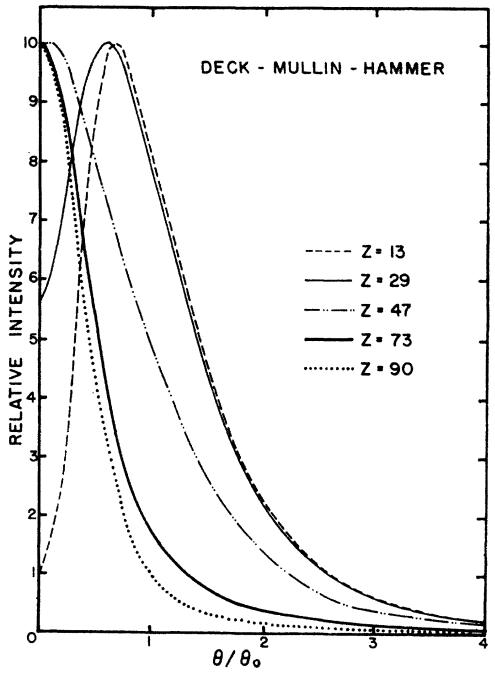

FIG. 4. The angular distributions of photons at the high-frequency limit according to the expression of Deck, Mullin, and Hammer.

[30] T. J. Keegan, Rev. Sci. Instr. 24, 472 (1953).

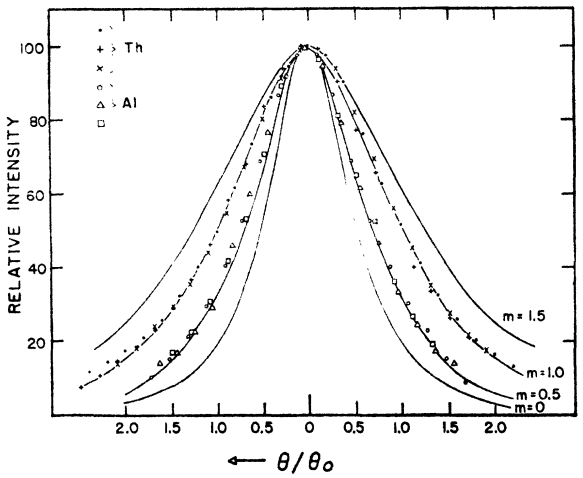

FIG. 5. Horizontal x-ray intensity distributions from thorium and aluminum for electrons having a total energy of 16.8 MeV. The experimental measurements shown here with different symbols were taken over periods of several days to determine that the distributions do not change with time. The solid curves represent the expected angular distributions of photons by electrons of total energy E_0 incident upon targets of different thicknesses as specified by the parameter m.

The long-pulse circuits were used to produce yield pulses of about 20 μsec duration. The variable delay was used to initiate the expander current and the delay was adjusted so that the yield pulse would straddle the 90-deg point in phase where the magnetic field in the betatron passes through its maximum. In this way the energy spread associated with the sinusoidal time dependence of the magnetic field was minimized. For this mode of operation the betatron amplitude was electronically regulated by means of a series impedance device which maintained the energy within about ± 40 keV. This mode of operation was especially useful in the forward beam where the intensity was high and it was necessary to reduce, or check for, excessive pileup in the counting equipment.

C. Beam Monitors

The collimated x-ray beam was monitored by means of a large ionization chamber with a thick aluminum converter. The charge collected from the chamber was integrated on a condenser and the voltage measured by means of a vibrating reed electrometer.

The ionization chamber used in the Z-dependence section of the experiment had an active volume consisting of two sections giving a total cylindrical volume of 11.43 cm in diameter and 5 cm deep. The converter for this chamber was 4 in. of aluminum. This chamber was operated at a potential of 135 V and was so placed as to intercept the beam through the polystyrene scatterer.

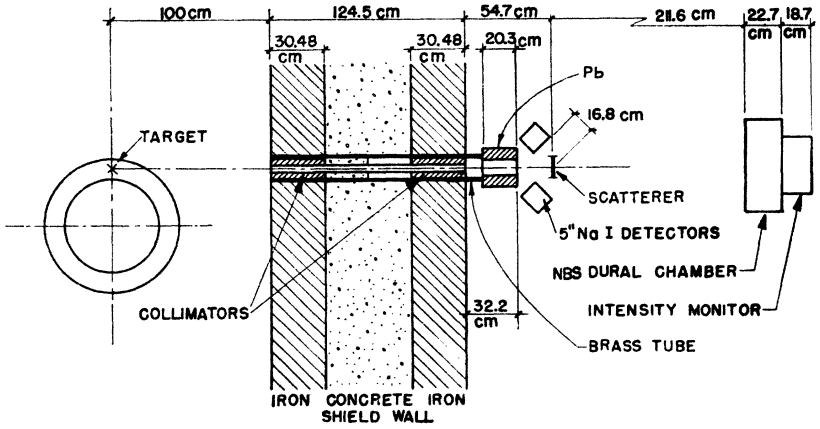

FIG. 6. The second experimental arrangement. This is the physical layout used during the more extensive measurements made with the thorium target.

In the work on the anomalous polarization and the angular distribution measurements from thorium, the total yield was measured using the same arrangement with the exception that the ionization chamber was replaced by a copy of the standard monitor of the National Bureau of Standards.[31]

Two additional monitors were used in the second part of the research. One was an ionization chamber mounted behind the N.B.S. chamber used to monitor the beam intensity through the scatterer so that it could be maintained constant during a complete run at a given angle. The other was a transmission ion chamber used to monitor the central intensity as a check on the angular distribution.

D. Physical Layout of the Experiment

In the first experiment on the survey of the Z dependence at 0° the experimental arrangement was much the same as that used in the previous work.[27] The beam was hardened by passing through 27.7 g/cm² of beryllium and then collimated to a full angular spread of 0.5°. The beam then passed through the 1.93 g/cm² carbon scatterer into the 4 in. of aluminum and the ionization chamber of the monitor. The two photomultipliers were placed such that their center lines lay 135° back from the 0° beam. The front surfaces of the NaI scintillators were 6.625 in. away from the center of the carbon scatterer.

The second arrangement used in the more detailed investigation of the radiation from thorium differed from the first primarily because a new shield wall had been built and it was convenient to use a slightly larger beam. This layout is shown in Fig. 6. The beam was hardened by 18.3 g/cm² of beryllium and was collimated to a full angle of 1° forming a square 5 cm on a side at the position of the carbon scatterer 280 cm from the betatron target.

In the check for anomalous polarization the photomultipliers were mounted in a rotatable frame at 90° to the direction of the beam.

E. Detection System

The detection system made use of the resonance scattering of 15.1-MeV photons for the measurement of the number of 15.1-MeV photons in the electron bremsstrahlung spectrum. The scattered photons were detected by means of two NaI crystals 5 in. in diameter and 4 in. thick which were optically sealed to 7046 photomultipliers by means of Dow Corning No. 200 fluid. Mounted on the front of each crystal was a radioactive Na^{22} source for the purpose of checking the gain of the detector system. The use of two photomultipliers doubled the solid angle and hence the counting rate and had the meritorious effect of decreasing the variation in sensitivity to scattering from different parts of the scatterer.

The pulses from the photomultipliers passed through 11.5 to 1 attenuators, or passed directly to Hewlett Packard 460A amplifiers, through biased diode discriminators to the grid of a cathode follower mixing circuit, and into the 100-channel analyzer, as shown in Fig. 7. Pulses entering the mixing circuit were shaped by 5 m shorted lines and clipped by biased diodes before being added at the grid of the cathode follower. This circuit placed right after the fast amplifiers reduced the length of the input pulses and eliminated all pulses less than about 4 MeV by means of the biased diode. It also acted as a pulse stretcher with an output suitable for the analyzer.

The 100-channel analyzer was gated on for about 5 and 30 μsec, respectively, for the short- and long-pulse runs. The gating was accomplished by a variable time delayed gate which was triggered by the betatron expander pulse and was so adjusted as to give a gate which encompassed the yield pulse.

The gains of the two individual channels of the detector system, A and B, were set separately using pulses from the Na^{22} source. A minor check of the

[31] J. S. Pruitt and S. R. Domen, National Bureau of Standards Report No. 6218, NBS Monograph 48, June, 1962 (unpublished).

electronics was made at frequent intervals during the investigations and consisted of checking each channel, one at a time, to make sure that the Na^{22} photopeak had not shifted.

The angle between the 0° beam and the collimator was determined by placing an x-ray film in the beam and determining the position of the beam center relative to the collimator entrance. This position could be determined to ± 1 mm at 1 m where $\theta_0 = 3.27$ cm at this distance. The beam seemed to move with energy by as much as 5 mm or $0.15\,\theta_0$.

The angle at which the isochromat was to be measured was changed by lowering the betatron on to the tracks and rotating the whole machine. This had the advantage of leaving the target and beam stopper unchanged throughout the experiment. As an added precaution against changes in the operating conditions, the angular distribution of the intensity was measured at the start and finish of each run but no important changes were found.

IV. EXPERIMENTAL RESULTS

A. Survey of the Forward Yields

The experimental yields of 15.1-MeV gamma rays scattered from a collimated x-ray beam at zero deg were measured as a function of electron energy for Al, Cu, Pd, Ta, and Th using the first experimental arrangement.

The length of a typical run was determined by the time to collect a definite charge on the ionization chamber, usually 0.8 V on a 0.01-μF polystyrene capacitor, and occupied about 10 min. During this time, of the order of 100 useful counts were recorded in appropriate channels in the 100-channel analyzer. A

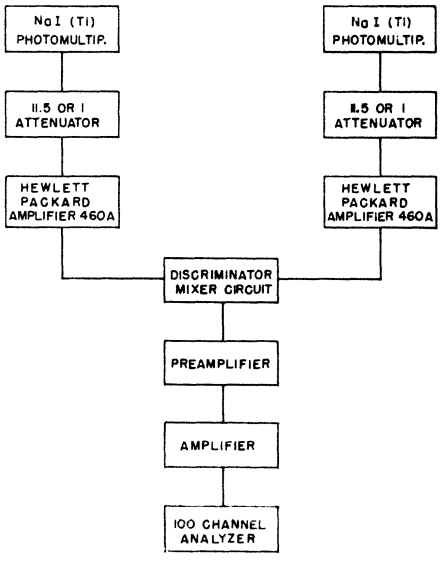

FIG. 7. Block diagram of the electronic circuits.

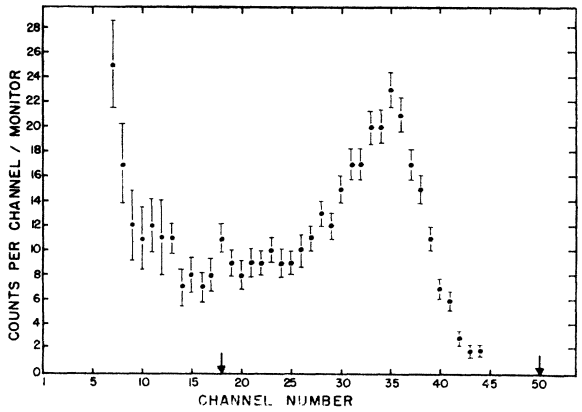

FIG. 8. Pulse-height spectrum from scattered gamma rays. This pulse-height spectrum was obtained by subtracting the average background (averaged over three runs below 15.1 MeV) from the average number for 12 runs above 15.1 MeV.

composite pulse-height spectrum of the sum of the pulses from the two NaI crystals from the average of 12 runs is shown in Fig. 8. The total background in the channels 25–50 was generally less than one count arising from cosmic rays but became about 2 counts for long-pulse runs where the gate length was about 30 μsec.

The selection of channels 18–50 about doubled the background but the lower limit was chosen since it increased the counted number of events and rendered the result less dependent on the stability of the amplifier and discriminator system.

In the region near the high-frequency limit of the spectrum, the energy was changed by intervals of about 10 keV and back from the tip by intervals of about 500 keV. The pulse-height spectrum corresponding to a given flux of energy through the carbon scatterer, as determined by the monitor, was recorded for each run. The net count under each of these spectra was determined for a number of targets in the betatron. The forward yields obtained for various elements are shown in Fig. 9. The yields are normalized to the same total energy passing through the scatterer as measured by the thick-walled monitor and are shown as functions of the kinetic energy of the electrons incident on the targets. The strong increase in the threshold yield with Z is clearly shown. The theoretical yield as calculated from the Bethe-Heitler theory for the forward direction, using formula ($2BN$) of reference 4, is shown for comparison. The curve shown for $m = 0.6$ includes the effect of multiple scattering but it is not significantly different from that for an infinitesimally thin target ($m = 0$). The curve is normalized to the aluminum data at 17.5 MeV.

B. Isochromat Yields at Several Angles from Thorium

The more extended measurements on thorium were made about a year after the survey, using the arrange-

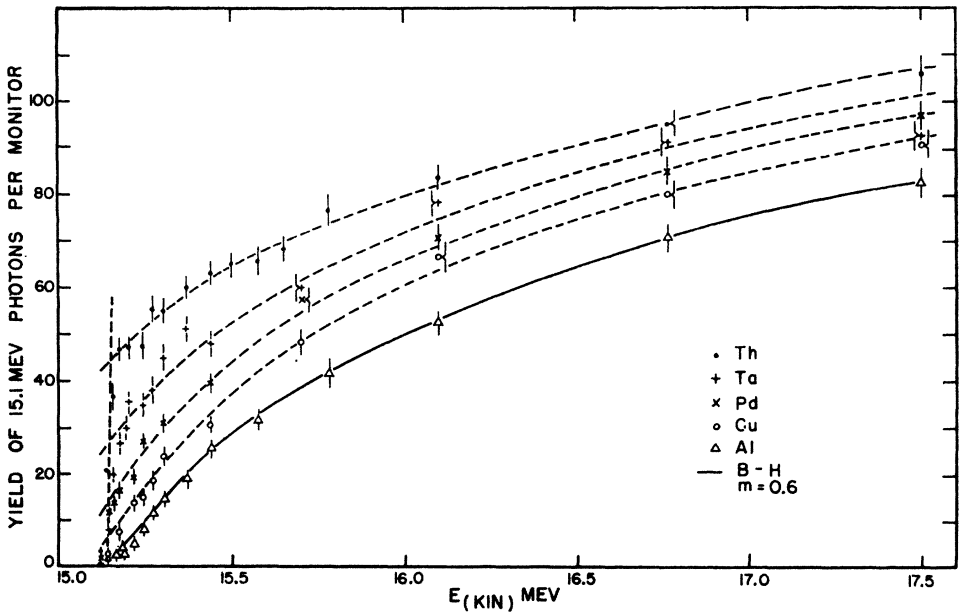

FIG. 9. The 0° isochromats from the survey of elements. Shown in the figure are the forward yields of 15.1-MeV photons per unit total energy of x-rays passing through the scatterer as a function of the kinetic energy of the impinging electrons. The solid line represents the forward yield as calculated by the Bethe-Heitler (B-H) formula for an $m=0.6$ target. It is normalized to the aluminum yield at 17.5 MeV.

ment of Fig. 6 described in the previous section. In this arrangement the betatron could be rotated so that the x-ray beam selected by the collimator through the shield was at different angles with respect to the direction of the electrons striking the target. The total-angular width of the square collimator was 1° corresponding to $\pm 0.28\ \theta_0$ at the threshold energy. This angular resolution was much better than that introduced by multiple scattering in the target.

The thorium target and the experimental procedure were the same as that used in the survey. The yields were again obtained for a given energy flux of gamma rays passing through the sample. The yields at various angles are shown in Figs. 10 and 11 on the same absolute scale. It can be seen that the scattering yields as a function of energy are very similar at all angles and that there are no sharp anomalies near the threshold. The yield at 0.8 θ_0 is about 5% above those at 0.1 θ_0 and 1.6 θ_0 and 30% above that at 3.1 θ_0. A separate check on the angular distribution was made at 16.1 MeV by varying the position along the orbit at which the internal target intercepts the beam. In this case the maximum was found at 0.74 θ_0 with a yield of 11% above the average at 0.1 θ_0 and 1.5 θ_0. Although the latter method indicates a slightly stronger variation the results agree within the statistical accuracy of these runs. Both methods indicate that the angular distribution of the tip photons is only slightly different than the total x-ray spectrum as represented in Fig. 5.

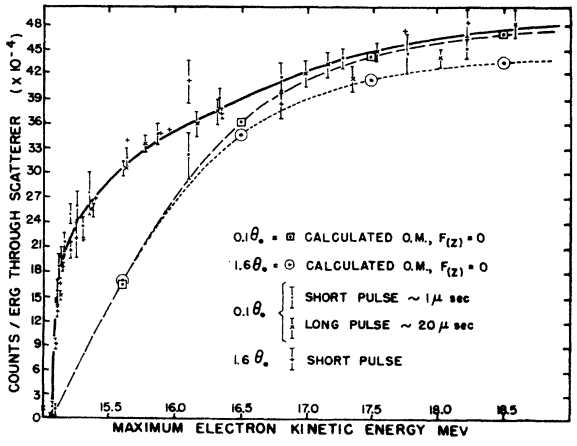

FIG. 10. The 15.1-MeV yields from the thorium target at various angles. The solid curve through the experimental points is arbitrary. The dashed curves connect points obtained using the Olson-Maximon (O.M.) differential spectrum $[f(Z)=0]$. These are normalized to the same total energy through the scatterer at each energy and angle.

In order to obtain the intensity of the 15.1-MeV isochromat corresponding to the spectrum integrated over the angle, it is necessary to take an appropriate average of the data obtained at the different angles. This was accomplished by assigning to the points measured at each angle an angular interval of coverage defined by the midpoints between it and the next angle at which measurements were made and averaging the observed yields with a weighting factor proportional to the yield into the solid angle corresponding to that angular interval. For this purpose the yield as a function of angle was based on the observations shown in Fig. 5. This averaged yield as a function of energy is not very different from those at particular angles.

An over-all efficiency for the detector system is obtained by equating the observed counts/erg for the total spectrum to the calculated number of 15.1-MeV photons per MeV energy interval in a 17.5-MeV Bethe-Heitler spectrum integrated over all angles and normalized to one erg of total energy after corrections for

the absorption by the beryllium and other materials in the beam. This efficiency was found to be 2.36×10^{-6} MeV and can be considered as the energy width that is effective in producing counts in the detector system.

This over-all efficiency is used in calculating the theoretically expected yields at the different angles shown in Figs. 10 and 11. Any systematic error in the flux measurement between different angles cancels out since the detection arrangement was unchanged. The accuracy of the resulting calibration thus depends only on the reliability of the assumed spectrum shape. The shape is clearly not quite correct at the tip but the ratio of the 15.1 MeV isochromat to the total energy in the spectrum is expected to be correct within 5% at 17.5 MeV.

An attempt was made to calculate the over-all absolute efficiency but the result was about a factor of two larger than that found experimentally. It was, however, subject to errors in several factors and the lack of agreement suggests that there was a large error in one of them.

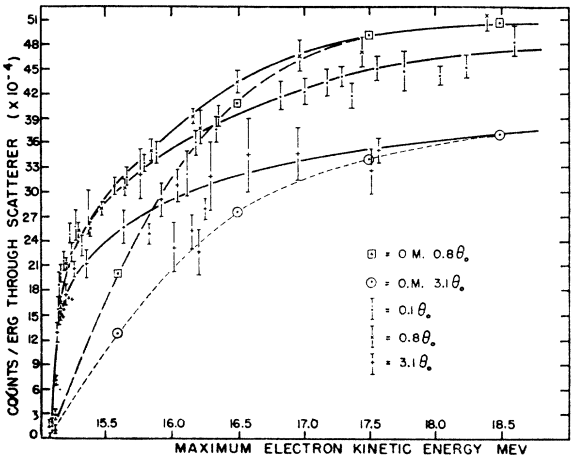

FIG. 11. The 15.1-MeV isochromat from thorium at various angles. The solid curves are arbitrarily drawn to connect the data points while the dashed curves connect points obtained from the Olson-Maximon [$f(Z)=0$] differential spectrum and the efficiency of the counting system.

C. Linear Polarization of Photons at the Tip

An attempt to detect a linear polarization was made at an angle of 3.0 ± 0.4 deg ($1.6\ \theta_0$) to the forward direction, by observing the ratio of photons scattered vertically to those scattered horizontally. The data are summarized in Table I. Some data were taken at two energies, $T=15.18$ MeV and $T=16.1$ MeV, although the accuracy is not high at either. The background from photons less than 15.1 MeV was small and isotropic for the two positions. The data show no asymmetry outside of statistics and do not indicate any strong anomalous polarization.

Only small polarizations are expected at this energy. From the calculations of Fronsdahl and Überall one obtains, for $1.6\ \theta_0$, polarization ratios ($\sigma_\perp/\sigma_{||}$) of 1.04 for $k/T=0.899$ and 0.90 for $k/T=0.999$. One may note that the well-known Sauter formula for the photoeffect gives a similar ratio for photons of 15.1 MeV.[9] The experimental ratios 1.05 and 0.98 are in reasonable agreement with calculations and do not indicate any anomalies in the polarization at the high-frequency limit.

V. COMPARISON OF THEORY AND EXPERIMENT

The 15.1-MeV yields from several elements at 0° are shown as a function of electron energy in Fig. 9. It is difficult to compare these experimental results with calculations. Although the Bethe-Heitler theory does represent very well the yield from a low-Z element such as aluminum, it is apparent that it does not represent the yields from high-Z elements near the high-frequency limit.

Calculations which are valid only near this limit have been referred to previously, and others which are valid several MeV from the tip can be used to predict the ratio of the cross sections at the threshold and at 17.5 MeV. The ratio of the D.M.H. cross section at 0° to the forward Bethe-Heitler cross section, for 15.1-MeV photons from electrons having kinetic energies of 17.5 MeV, can be expressed as

$$\frac{\sigma_{\text{tip}}}{\sigma^{17.5}}=3.35(\alpha Z)^3 e^{-\pi\alpha Z}F(\gamma)\frac{P(E)}{P(\infty)}, \tag{9}$$

where the constant 3.35 is determined for $k/E_0=0.84$ and the other symbols are those defined following Eq. (8). The Bethe-Heitler cross section used was that given as formula (2BN) of reference 4. The ratio multiplied by $(18.0/15.6)^3$ to account for the monitor response at the two energies is shown as the solid line in Fig. 12. It shows a dominant Z^3 dependence. The experimental points shown in the figure represent the ratio of the extrapolated yield at the threshold to that at 17.5 MeV from Fig. 9.

The experimental angular distributions and the forward yields are considerably modified by the multiple scattering of the electrons in the target. In order to be comparable with the experimental results, the theoretical photon distributions were folded into the angular distributions of electrons in the target as

TABLE I. Polarization measurements.

Position of counters	Total counts $k/T=0.996$	Total counts $k/T=0.96$
Vertical	644 ±25	378 ±19
Horizontal	656 ±25	360 ±19
Ratio	0.98± 0.08	1.05± 0.1

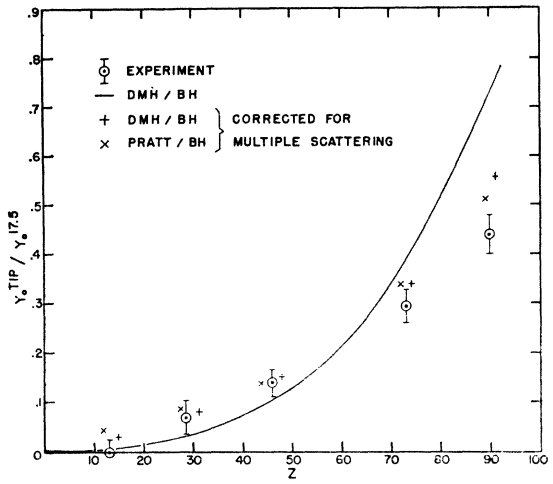

FIG. 12. The ratio of the observed forward yields at threshold to that at 17.5 MeV. The solid line represents the ratio of the calculated forward yields neglecting the effect of multiple scattering. The symbols (+) and (×) represent the calculated points as modified by multiple scattering. These are displaced from the correct Z coordinate in order to display them without superposition.

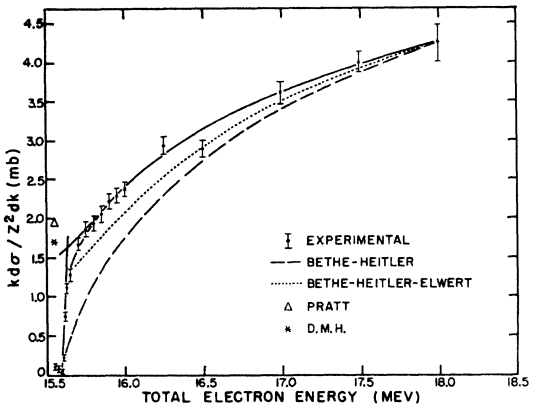

FIG. 13. Comparison of experimental and calculated values of $kd\sigma/Z^2dk$. The experimental points are normalized to the Bethe-Heitler calculation at 18.0-MeV total energy. The two values at the extreme left represent the tip values as calculated by inverse photoeffect by Pratt and an evaluation of the tip cross section by Deck, Mullin, and Hammer.

determined from the observed value of m for each target. The specific theoretical values shown in the figure were obtained using the tip yields and angular distributions of Figs. 1, 3, and 4.

One may note that the multiple scattering reduces the forward yield from thorium, while it increases the yield from light elements. The experimental points are somewhat below the corrected calculations, especially for the heavy elements. The differences could be attributed to the inaccuracies in the fundamental differential cross sections used or to errors associated with multiple scattering.

The experimental yield of 15.1-MeV photons in the integrated over angle bremsstrahlung spectrum from thorium is the most reliable and is also the most easily compared with calculations. The yield per erg has been reduced to a cross section by multiplying by the calculated energy incident on the monitor per electron and normalizing to the Bethe-Heitler value of 4.24 mb for the expression $(kd\sigma/Z^2dk)$ for 15.1-MeV photons from a 17.5-MeV spectrum. This cross section is shown in Fig. 13 against the total electron energy.

An extrapolation of the experimental values to the threshold leads to a value of 1.61 ± 0.16 mb for the cross section at the high-frequency limit of a 15.1-MeV spectrum. This may be compared to a value of 1.96 mb based on the work of Pratt[32] and a value of 1.74 mb as obtained from the work of Deck, Mullin, and Hammer using the value of 1.3 from their expression for extreme relativistic energies and the energy dependence given by Pratt.

It is apparent that the calculations at the high-frequency limit are in reasonable agreement with the experimental observations even though the accuracy of the calculations are not expected to be very great for an atomic number as high as 90.

The transition back from the tip seems to be gradual for all angles and falls in with the Born approximation curves about 2 MeV above the threshold in each case. The correction of the Bethe-Heitler cross section by means of the Elwert factor[4,7] produces a curve of about the right shape but is not sufficient to remove the discrepancy at the tip as indicated in the figure. The integrated cross section at the tip is shown in Fig. 1 together with curves calculated from theory. Also shown in this figure are the values for the integrated tip cross section given by Fano, Koch, and Motz.[3] Measurements at this energy have been limited to high Z and it would be interesting to have measurements of the integrated yields from the lighter elements.

The calculated points for the theoretical curves in Figs. 10 and 11 are those obtained using the Olson-Maximon differential cross section with $f(Z)=0$. The calculated and experimental points given in these figures at energies well above the threshold are directly comparable since the calculated values are normalized to the efficiency obtained from the integrated Bethe-Heitler cross section at 17.5-MeV kinetic energy. The agreement is good in the region where the calculations are expected to apply. It can be seen that the excitation functions for the 15.1-MeV isochromat at the different angles are all quite similar in shape but differ somewhat in magnitude. Thus, the observed angular dependence

[32] The values indicated as based on Pratt are derived from his earlier published work and have not been changed to agree with the more recent calculations of R. J. Jabbur and R. H. Pratt, Phys. Rev. 129, 184 (1963). Their analytic expression agrees with D.M.H. below $Z=50$. For $Z=90$ their calculations cover a range of values extending from that given by D.M.H. to 35% higher.

near the high-frequency limit is very similar to that for photons well below the limit as is expected from the calculations for high-Z elements. The distribution, however, is dominated by multiple scattering to such an extent that it does not reveal very well the narrower intrinsic distribution near the threshold. No attempt is made to determine the basic angular distributions. It would be desirable to extend these measurements to include thin-target angular distributions from light as well as heavy elements.

ACKNOWLEDGMENTS

The authors would like to express their appreciation to J. Kanz and H. Moore for their assistance in taking the data; to Mrs. E. Hutchesin and M. Suhre, Jr., for coding and evaluating the Olson-Maximon equations for the experimental angles using the IBM 650; and to Mrs. F. Kuchnir for evaluating the theoretical expressions for the angular distributions. They are particularly indebted to Dr. R. H. Pratt for communications with respect to the theory.

PHYSICAL REVIEW VOLUME 129, NUMBER 5 1 MARCH 1963

Gamma Rays from the $Be^9(\alpha,n_1)C^{12}$ Reaction*

J. B. SEABORN,† G. E. MITCHELL,‡ N. R. FLETCHER, AND R. H. DAVIS
Department of Physics, Florida State University, Tallahassee, Florida
(Received 17 September 1962)

The excitation function of the 4.43-MeV gamma ray from the $Be^9(\alpha,n_1\gamma_{4.43})C^{12}$ reaction has been studied and angular distributions have been measured at 13 alpha-particle energies from 3.6 to 7.6 MeV in an effort to determine compound nucleus nature of the $Be^9+\alpha$ system. Many broad resonances are found in the energy region studied.

INTRODUCTION

THE $Be^9(\alpha,n)$ reaction is of current interest to many investigators because of the possibility of a successful description of the reaction mechanism as a direct process. The applicability of a direct interaction theory depends on the amount of compound nucleus contribution in the reaction amplitude. We have studied the resonance structure of one exit channel of the $Be^9+\alpha$ system by observing the 4.43-MeV gamma ray emitted in the de-excitation of the C^{12} first excited state. This reaction has been studied extensively below 5.3 MeV,[1] and (n,γ) angular correlations have been measured at $E_\alpha=3.35$ MeV [2] and 5.35 MeV.[3] These results have yielded information about possible reaction mechanisms.

In the present work the excitation function of the 4.43-MeV gamma ray is extended to $E_\alpha=10$ MeV. The $Be^9(\alpha,n,\gamma_{4.43})C^{12}$ reaction cross section decreases rapidly above 5.5 MeV in contrast to the previously reported rise in the total neutron cross section.[4] Reactions other than those leading to C^{12*} which can contribute to the increasing neutron yield are:

$$Be^9+\alpha \rightarrow Be^8+\alpha+n, \quad (1)$$

$$\rightarrow Be^9+\alpha \rightarrow Be^8+n+\alpha, \quad (2)$$

$$\rightarrow Be^8+He^5 \rightarrow Be^8+\alpha+n, \quad (3)$$

$$\rightarrow 3\alpha+n. \quad (4)$$

These reactions will produce a low-energy continuum of neutrons. Such a low-energy neutron group was first observed by Auger[5] in 1933 in a study of neutrons from a Po-Be source. A few years later Bjerge[6] established that these slow neutrons were not accompanied by gamma rays. The results from these experiments were questioned,[7] and only recently has the existence of the low-energy neutrons been confirmed by Romain *et al.*[8] and by the present work in conjunction with previous results. At higher bombarding energies a neutron continuum has been observed by Nilsson and Kjellman.[9]

EXPERIMENTAL PROCEDURE AND RESULTS

The alpha-particle beam[10] of the Florida State University Tandem Van de Graaff Accelerator was used to bombard a thin beryllium target prepared by vacuum

* Supported in part by the Air Force Office of Scientific Research.
† Present address: Department of Physics, University of Virginia, Charlottesville, Virginia.
‡ Present address: Pegram Nuclear Physics Laboratory, Columbia University, New York.
[1] T. W. Bonner, A. A. Kraus, J. B. Marion, and J. D. Schiffer, Phys. Rev. **102**, 1348 (1956).
[2] J. Kjellman, T. Dazai, and J. H. Neiler, Nucl. Phys. **30**, 131 (1962).
[3] J. B. Garg and N. H. Gale (unpublished).
[4] J. H. Gibbons and R. L. Macklin, Phys. Rev. **114**, 571 (1959).
[5] P. Auger, J. Phys. Radium **4**, 719 (1933).
[6] T. Bjerge, Proc. Roy. Soc. (London) **A164**, 243 (1938).
[7] F. Ajzenberg and T. Lauritsen, Rev. Mod. Phys. **24**, 321 (1952).
[8] F. A. St. Romain, T. W. Bonner, R. L. Bramblett, and J. Hanna, Phys. Rev. **126**, 1794 (1962).
[9] A. Nilsson and J. Kjellman, Nucl. Phys. **32**, 177 (1962).
[10] G. E. Mitchell, E. B. Carter, and R. H. Davis, Bull. Am. Phys. Soc. **6**, 227 (1961).